Anisotropy in transport and magnetic properties of K_{0.64}Fe_{1.44}Se_{2}

Hechang Lei (□ □ □) and C. Petrovic

Phys. Rev. B **83**, 184504 — Published 11 May 2011

DOI: 10.1103/PhysRevB.83.184504

Anisotropy in transport and magnetic properties of $K_{0.64}Fe_{1.44}Se_2$

Hechang Lei (雷 和 畅) and C. Petrovic
Condensed Matter Physics and Materials Science Department, Brookhaven National Laboratory, Upton, New York 11973, USA
(Received 4 February 2011; revised manuscript received 1 April 2011; published xxxxx)

We report a study of the anisotropy in transport and magnetic properties of $K_{0.64}Fe_{1.44}Se_{2.00}$ single crystals. The anisotropy in resistivity is up by one order of magnitude between 1.8 and 300 K. The magnetic susceptibility exhibits weak temperature dependence in the normal state with no significant anomalies with decreasing temperature. The lower critical fields H_{c1} of $K_{0.64}Fe_{1.44}Se_{2.00}$ are only about 3 Oe and the anisotropy of $H_{c1,c}/H_{c1,ab}$ is about 1. The critical currents for $H \| ab$ and $H \| c$ are about 10–10^3 A/cm^2, which is smaller than in iron pnictides and in $FeTe_{1-x}Se_x$, and nearly isotropic.

DOI: 10.1103/PhysRevB.00.004500 PACS number(s): 74.70.Xa, 74.25.Sv, 74.25.Op

I. INTRODUCTION

The discovery of superconductivity in $LaFeAsO_{1-x}F_x$ has triggered intense research activity that resulted in the detection of critical temperatures up to 56 K in pnictide materials.[1–5] Soon after, several types of iron-based superconductors have been discovered, including AFe_2As_2 (A = alkaline or alkaline-earth metals, 122 type),[6,7] LiFeAs (111 type),[8] $(Sr_4M_2O_6)(Fe_2Pn_2)$ (M = Sc, Ti or V, 42622 type),[9,10] and α-PbO type FeSe (11 type).[11] The 11-type materials, FeSe, $FeTe_{1-x}Se_x$,[12] and $FeTe_{1-x}S_x$,[13] provided an example of iron-based superconductivity in a rather simple crystal structure without the charge reservoir layer. Yet, these simple binary structures share a square-planar lattice of Fe with tetrahedral coordination and similar Fermi surface topology with other iron-based superconductors.[14] Furthermore, 11-type superconductors contain some distinctive structural and physical features, such as interstitial iron $Fe_{1+y}Te$ and a significant pressure effect.[15–17] Under external pressure, T_c can be increased from 8 to 37 K and dT_c/dP can reach 9.1 K/GPa, the highest increase in all iron-based superconductors.[17] This behavior may be understood from an observation related to the anion height between Fe and As (or Se, Te) layers. There is an optimal distance around 1.38 Å with a maximum transition temperature $T_c \simeq 55$ K.[18] The anion height in FeSe decreases gradually with increasing temperature toward the optimal value, thereby increasing T_c.[18] Moreover, high upper critical fields and currents were observed in iron-based superconductors.[19–21]

Another method for tuning the anion height is the intercalation between FeSe layers, which can change both the local environment of Fe-Se tetrahedron and the average crystal structure. The intercalation can also decrease the dimensionality of conducting bands. The presence of low-energy electronic collective modes in layered conductors helps screen the Coulomb interaction, which may contribute constructively to superconductivity.[22] It is observed that in iron-based superconductors T_c increases from 11 type to 1111 type. Very recently T_c was raised in iron selenide materials to about 30 K by intercalating K, Rb, Cs, and Tl between the FeSe layers (AFeSe, 122 type),[23–29] as opposed to increasing the pressure. The intercalation of alkaline metals decreases Se height[28] and changes the average space group from P4/nmm in FeSe to I4/mmm in AFeSe, 122 type. The Fe-Se interlayer distances are expanded and may contribute to an electronic and magnetic dimensionality reduction. Furthermore, an insulator-superconductor transition (IST) can be induced by tuning the Fe stoichiometry in $(Tl_{1-x}K_x)Fe_{2-y}Se_2$ ($0 \leqslant x \leqslant 1, 0 \leqslant y \leqslant 1$).[29] This suggests that the superconductivity of AFeSe, 122 type, is in the proximity of a Mott-insulating state.[29] Thus, it is important to study electronic and magnetic anisotropy in normal and superconducting states in AFeSe, 122 type, in order to shed more light on the superconducting mechanism and possible symmetry of the order parameter.

In this work, we report the anisotropy in electronic transport and magnetization in the normal state of $K_{0.64(4)}Fe_{1.44(4)}Se_{2.00(0)}$ single crystals. We also present anisotropic parameters of the superconducting state.

II. EXPERIMENT

Single crystals of $K_xFe_2Se_2$ were grown by the self-flux method with nominal composition $K_{0.8}Fe_2Se_2$. Prereacted FeSe and K pieces (purity 99.999%, Alfa Aesar) were put into the alumina crucible and sealed into the quartz tube under a partial pressure of argon. The quartz tube was heated to 1030°C, kept at this temperature for 3 h, and then slowly cooled to 730°C at a rate of 6 °C/h. Platelike crystals up to $5 \times 5 \times 1$ mm^3 were grown. X-ray diffraction (XRD) spectra were taken with Cu K_α radiation ($\lambda = 1.5418$ Å) using a Rigaku Miniflex x-ray machine. The lattice parameters were obtained by fitting the XRD spectra using RIETICA software.[30] The elemental analysis was performed using an energy-dispersive x-ray spectroscopy (EDX) in a JEOL JSM-6500 scanning electron microscope. Electrical resistivity, $\rho(T)$, measurements were performed in a Quantum Design PPMS-9. The in-plane resistivity, $\rho_{ab}(T)$, was measured using a four-probe configuration on rectangularly shaped and polished single crystals with the current flowing in the ab plane of the tetragonal structure. The c-axis resistivity, $\rho_c(T)$, was measured by attaching current and voltage wires to the opposite sides of the platelike sample.[31,32] Since the sample surface is easily oxidized, sample manipulation in the air was limited to 10 min. The sample dimensions were measured with a Nikon SMZ-800 optical microscope with 10-μm resolution. Electrical transport and heat capacity measurements were carried out in the PPMS-9 from 1.8 to 300 K. Magnetization measurements were performed in a Quantum Design Magnetic Property Measurement System (MPMS) up to 5 T.

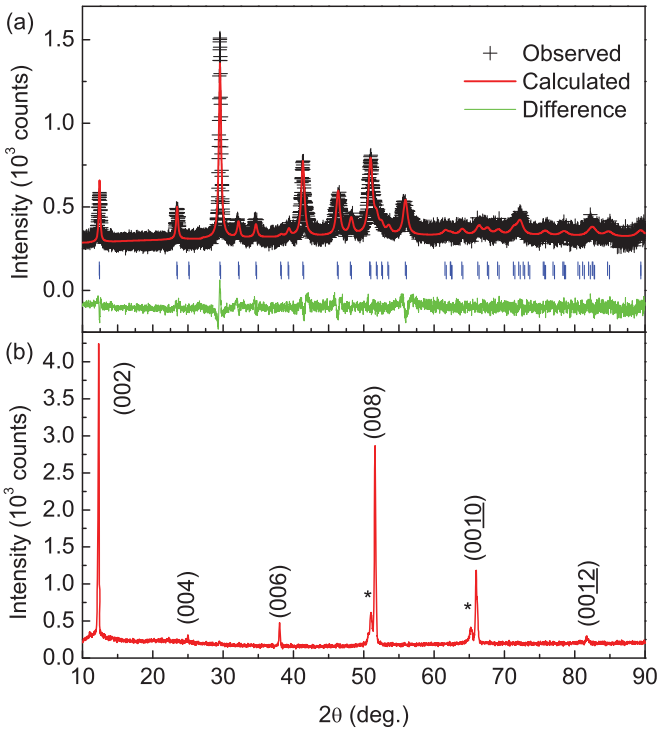

FIG. 1. (Color online) (a) Powder and (b) single-crystal XRD patterns of $K_xFe_{2-y}Se_2$, respectively.

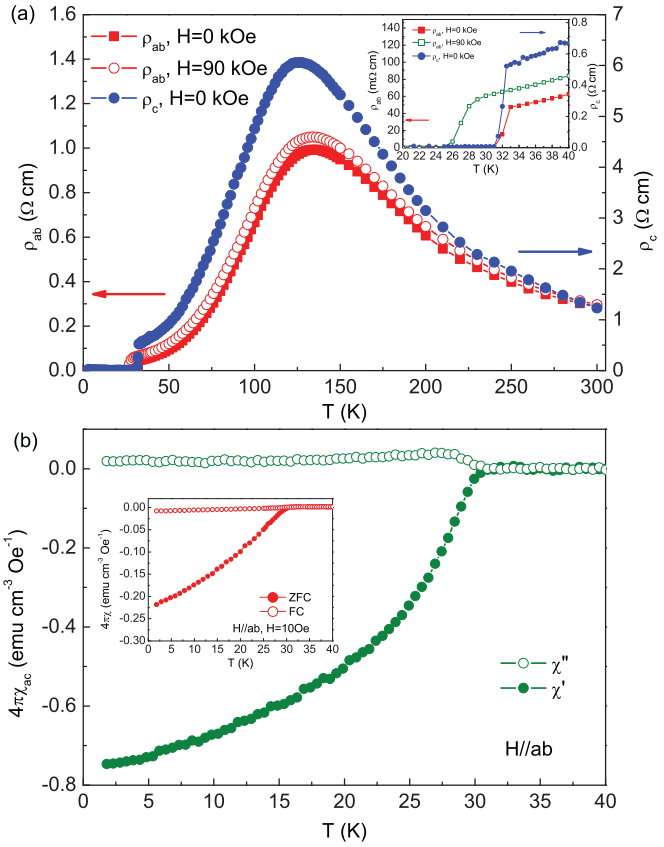

FIG. 2. (Color online) (a) Temperature dependence of the resistivity, $\rho_{ab}(T)$ and $\rho_c(T)$, of $K_xFe_{2-y}Se_2$ with and without $H = 90$ kOe along the c axis. Inset: Enlarged resistivity curve near T_c. (b) Temperature dependence of ac magnetic susceptibility of $K_xFe_{2-y}Se_2$ in $H_{ac} = 1$ Oe. Inset: Temperature dependence of dc magnetic susceptibility with zero-field cooling and field cooling.

III. RESULTS AND DISCUSSION

Figure 1(a) shows the x-ray diffraction results of the ground crystal. It demonstrates phase purity—there are no extrinsic peaks present. The powder pattern can be indexed in the I4/mmm space group with fitted lattice parameters $a = 0.39109(2)$ nm and $c = 1.4075(3)$ nm ($R_p = 2.272$ and $R_{wp} = 3.101$), which are consistent with reported results.[23–25] On the other hand, XRD spectra of a single crystal reveal that the crystal surface is normal to the c axis with the plate-shaped surface parallel to the ab plane [Fig. 1(b)]. Furthermore, there is another weak series of (00l) diffraction peaks (labeled by the asterisks) associated with the main peaks. These two distinct sets of reflections could arise from the inhomogeneous distribution of K atoms, which is also observed in other AFeSe-122 single crystals.[34,35] The average stoichiometry was determined from EDX by examination of multiple points in the crystals. The measured compositions are $K_{0.64(4)}Fe_{1.44(4)}Se_{2.00(0)}$ (noted as $K_xFe_{2-y}Se_2$), indicating a substantial number of K and Fe vacancies. We also measured the composition mapping using EDX. The results show that the spatial distribution of K, Fe, and Se is homogenous.

The main panel of Fig. 2(a) shows the temperature dependence of resistivity in zero field, from 1.9 to 300 K, for a current along the ab plane and the c axis. At higher temperatures, both $\rho_{ab}(T)$ and $\rho_c(T)$ show a metal-insulator transition with maximum resistivities at about 135 and 125 K, respectively. The resistivity maximum, $\rho_{\max}$, might be related to a scattering crossover arising from a structure or magnetic phase transition, and it is a typical behavior in AFeSe-122 systems.[23–29] Furthermore, the temperature dependence of $\rho_{\max}$ correlates with the iron deficiency in the crystals.[33] From our resistivity data in the normal state below 300 K, the ratio ρ_c/ρ_{ab} is about 4–12. The anisotropy is much smaller than in $(Tl,K)_xFe_{2-y}Se_2$ and $(Tl,Rb)_xFe_{2-y}Se_2$ systems, where ρ_c/ρ_{ab} equals 70–80 and 30–45,[29,34] respectively. On the other hand, both $\rho_{ab}(T)$ and $\rho_c(T)$ undergo a very sharp superconducting transition at $T_{c,\text{onset}} = 33$ K, shown in the inset of Fig. 2(a). At 90 kOe the resistivity transition width is broader and the onset of superconductivity shifts to 28 K. However, the $\rho_{\max}$ curve has no obvious shift in magnetic fields up to 90 kOe for current transport along both crystallographic axes.

Figure 2(b) shows the temperature dependence of the ac susceptibility of $K_xFe_{2-y}Se_2$ single crystal with $H \parallel ab$. A clear superconducting transition appears at $T = 31$ K. This is consistent with the resistivity results. The superconducting volume fraction is about 75% at 1.8 K, indicating bulk superconductivity in the sample. The broad transitions in χ' and χ'' indicate microscopic inhomogeneity. The inset in Fig. 2(b) shows the dc magnetic susceptibility for $H \parallel ab$ with zero-field cooling (ZFC) and field cooling (FC). Diamagnetism can be clearly observed in both measurements, and $T_{c,\text{onset}}$ is almost the same as that determined from the ac susceptibility. On the other hand, the magnetization measured with FC is very small, which is a common behavior in two-dimensional

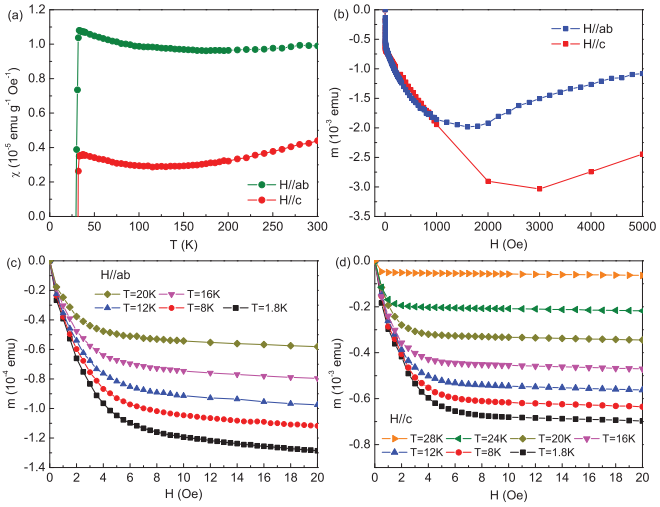

FIG. 3. (Color online) (a) Temperature dependence of magnetic susceptibility measured at 1 kOe for $K_xFe_{2-y}Se_2$ crystal with $H\|ab$ and $H\|c$. (b) Magnetization curve of $K_xFe_{2-y}Se_2$ at $T = 1.8$ K for $H\|ab$ and $H\|c$. (c) and (d) Low-field parts of $m(H)$ at various temperature for $H\|ab$ and $H\|c$, respectively.

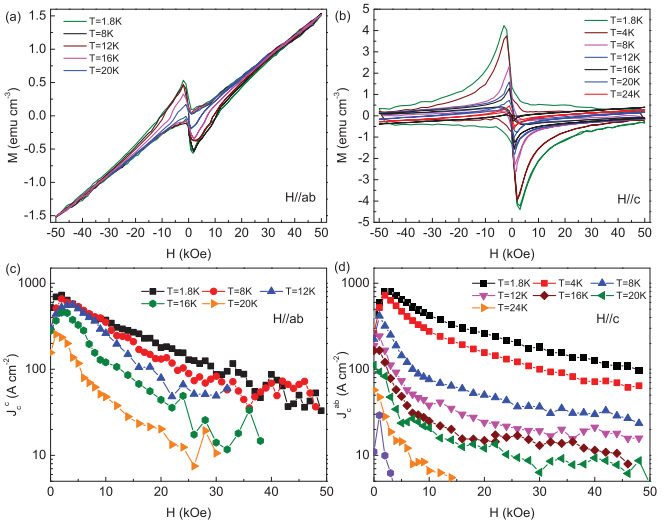

FIG. 4. (Color online) Magnetization hysteresis loops of $K_xFe_{2-y}Se_2$ for (a) $H\|ab$ and (b) $H\|c$. (c) In-plane and (b) interplane superconducting critical currents as determined from magnetization measurements using the Bean model.

superconductors, such as $(pyridine)_{1/2}TaS_2$[36] and Ni_xTaS_2.[37] The small magnetization values for FC is likely due to the complicated magnetic-flux-pinning effects in the layered compounds.[36]

The temperature dependence of magnetic susceptibility in the normal state is shown in Fig. 3(a) for $H\|ab$ and $H\|c$ with $H = 1$ kOe. A sudden drop at about 30 K corresponds to the superconducting transition. For $H\|c$, χ_c weakly decreases with temperature below 300 K and exhibits a weak upturn below 120 K. When the magnetic field is in the ab plane, χ_{ab} exhibits similar behavior but the minimum of susceptibility is located at about 175 K. The magnetic susceptibility enhancement with increase in temperature above 200 K is neither Pauli nor Curie-Weiss, suggesting the presence of magnetic interactions. This has been observed not only in other AFeSe-122 compounds[25,26,29,38] but also in $BaFe_2As_2$, and it is due to two-dimensional short-range antiferromagnetic (AFM) spin fluctuations.[39,40] The AFM interaction is, possibly, related to the Fe deficiency and is an intrinsic property of AFe_2Ch_2 (Ch = S, Se).

The initial dc magnetization versus field, $m(H)$, at $T = 1.8$ K for both directions is shown in Fig. 3(b). The shape of the $m(H)$ curves points to the fact that $K_xFe_{2-y}Se_2$ is a typical type-II superconductor. The peak in $m(H)$ is about 2 kOe for $H \parallel c$, consistent with the previous report.[23] However, it should be noted that H_{c1} is often much smaller than the peak value seen in the $m(H)$ curve. In $K_xFe_{2-y}Se_2$, the $m(H)$ curve deviates from linearity at a much lower field. The enlarged parts are shown in Figs. 3(c) and 3(d). The value of H_{c1} is usually determined by the field where the M-H curve deviates from the linear relation.[41] However, small H_{c1} introduces a significant error, so it is hard to evaluate $H_{c1}(0)$ using $H_{c1}(T) = H_{c1}(0)[1 - (T/T_c)^2]$. The approximate $H_{c1,ab}(T = 1.8\ \text{K})$ and $H_{c1,c}(T = 1.8\ \text{K})$ are 3.0(5) Oe.

Figures 4(a) and 4(b) show the magnetization loops for $H\|c$ and $H\|ab$ with the field up to 50 kOe. The paramagnetic background exists for both directions and is more obvious for $H\|ab$. This paramagnetic background originates from the nonsuperconducting fraction. The shapes of $M(H)$ and $M(T)$ (Fig. 3) are typical of type-II superconductors with some electromagnetic granularity.[42,43] The critical current is determined from the Bean model.[44,45] For a rectangular-shaped crystal with dimension $c < a < b$, when $H\|c$, the in-plane critical current density $J_c^{ab}(H)$ is given by

$$J_c^{ab}(H) = \frac{20\Delta M(H)}{a(1 - a/3b)},$$

where a and b ($a < b$) are the in-plane sample sizes in centimeters, $\Delta M(H)$ is the difference between the magnetization values for increasing and decreasing fields at a particular applied field value measured in emu/cm^3, and $J_c^{ab}(H)$ is the critical current in A/cm^2. It should be noted that the paramagnetic background has no effect on the calculation of $\Delta M(H)$. The situation is more complex when $H\|ab$. There are two different current densities: the vortex motion across the planes, $J_c^c(H)$, and that parallel to the planes, $J_c^{\|}(H)$, and, usually, $J_c^{\|}(H) \neq J_c^{ab}(H)$. Assuming $a,b \gg (c/3) \cdot J_c^{\|}(H)/J_c^c(H)$,[45] we can obtain $J_c^c(H) \approx 20\Delta M(H)/c$. The magnetic field dependence of $J_c^c(H)$ and $J_c^{ab}(H)$ is shown in Figs. 4(c) and 4(d). It can be seen that the critical current decreases with the applied field and the ratio of $J_c^c(H)/J_c^{ab}(H)$ is approximately 1. The critical current densities for both directions are 10–10^3 A/cm^2, which are much smaller than those of $BaFe_{2-x}Co_xAs_2$ in the same temperature range.[46]

IV. CONCLUSION

In summary, we have presented anisotropic transport and magnetic properties of $K_{0.64(4)}Fe_{1.44(4)}Se_{2.00(0)}$ single crystals

with $T_{c,\text{onset}} = 33$ K and without iron impurities. The resistivity anisotropy is much smaller than in other *A*FeSe-122 compounds. The magnetization decreases in the normal state with decreasing temperature from 300 K; this suggests the presence of AFM interactions. The lower critical fields, H_{c1}, are only about 3 Oe at 1.8 K and the anisotropy of $H_{c1,c}/H_{c1,ab}$ is about 1. The critical current values are isotropic and about $10–10^3$ A/cm^2 for both directions below 50 kOe.

ACKNOWLEDGMENTS

We thank John Warren for help with scanning electron microscopy measurements. The work at Brookhaven National Laboratory is supported by the the US Department of Energy (DOE) under Contract No. DE-AC02-98CH10886 and in part by the Center for Emergent Superconductivity, an Energy Frontier Research Center funded by the US DOE, Office for Basic Energy Science.

[1] Y. Kamihara, T. Watanabe, M. Hirano, and H. Hosono, J. Am. Chem. Soc. **130**, 3296 (2008).

[2] X. H. Chen, T. Wu, G. Wu, R. H. Liu, H. Chen, and D. F. Fang, Nature (London) **453**, 761 (2008).

[3] G. F. Chen, Z. Li, D. Wu, G. Li, W. Z. Hu, J. Dong, P. Zheng, J. L. Luo, and N. L. Wang, Phys. Rev. Lett. **100**, 247002 (2008).

[4] Z. A. Ren, J. Yang, W. Lu, Y. Wei, X. L. Shen, Z. C. Li, G. C. Che, X. L. Dong, L. L. Sun, F. Zhou, and Z. X. Zhao, Europhys. Lett. **82**, 57002 (2008).

[5] H.-H. Wen, G. Mu, L. Fang, H. Yang, and X. Y. Zhu, Europhys. Lett. **82**, 17009 (2008).

[6] M. Rotter, M. Tegel, and D. Johrendt, Phys. Rev. Lett. **101**, 107006 (2008).

[7] G. F. Chen, Z. Li, G. Li, W. Z. Hu, J. Dong, X. D. Zhang, P. Zheng, N. L. Wang, and J. L. Luo, Chin. Phys. Lett. **25**, 3403 (2008).

[8] X. C. Wang, Q. Q. Liu, Y. X. Lv, W. B. Gao, L. X. Yang, R. C. Yu, F. Y. Li, and C. Q. Jin, Solid State Commun. **148**, 538 (2008).

[9] H. Ogino, Y. Matsumura, Y. Katsura, K. Ushiyama, S. Horii, K. Kishio, and J. Shimoyama, Supercond. Sci. Technol. **22**, 075008 (2009).

[10] X. Y. Zhu, F. Han, G. Mu, P. Cheng, B. Shen, B. Zeng, and H.-H. Wen, Phys. Rev. B **79**, 220512(R) (2009).

[11] F. C. Hsu *et al.*, Proc. Natl. Acad. Sci. USA **105**, 14262 (2008).

[12] K.-W. Yeh *et al.*, Europhys. Lett. **84**, 37002 (2008).

[13] Y. Mizuguchi, F. Tomioka, S. Tsuda, T. Yamaguchi, and Y. Takano, Appl. Phys. Lett. **94**, 012503 (2009).

[14] A. Subedi, L. Zhang, D. J. Singh, and M. H. Du, Phys. Rev. B **78**, 134514 (2008).

[15] L. J. Zhang, D. J. Singh, and M. H. Du, Phys. Rev. B **79**, 012506 (2009).

[16] Y. Mizuguchi, F. Tomioka, S. Tsuda, T. Yamaguchi, and Y. Takano, Appl. Phys. Lett. **93**, 152505 (2008).

[17] S. Medvedev *et al.*, Nature Mater. **8**, 630 (2009).

[18] Y. Mizuguchi, Y. Hara, K. Deguchi, S. Tsuda, T. Yamaguchi, K. Takeda, H. Kotegawa, H. Tou, and Y. Takano, Supercond. Sci. Technol. **23**, 054013 (2010).

[19] H. Q. Yuan, J. Singleton, F. F. Balakirev, S. A. Baily, G. F. Chen, J. L. Luo, and N. L. Wang, Nature (London) **457**, 565 (2009).

[20] A. Yamamoto *et al.*, Appl. Phys. Lett. **94**, 062511 (2009).

[21] T. Kida, T. Matsunaga, M. Hagiwara, Y. Mizuguchi, Y. Takano, and K. Kindo, J. Phys. Soc. Jpn. **78**, 113701 (2009).

[22] A. Bill, H. Morawitz, and V. Z. Kresin, Phys. Rev. B **68**, 144519 (2003).

[23] J. Guo, S. Jin, G. Wang, S. Wang, K. Zhu, T. Zhou, M. He, and X. Chen, Phys. Rev. B **82**, 180520(R) (2010).

[24] Y. Mizuguchi, H. Takeya, Y. Kawasaki, T. Ozaki, S. Tsuda, T. Yamaguchi, and Y. Takano, Appl. Phys. Lett. **98**, 042511 (2011).

[25] J. J. Ying *et al.*, e-print arXiv:1012.5552.

[26] A. F. Wang *et al.*, Phys. Rev. B **83**, 060512(R) (2011).

[27] C.-H. Li, B. Shen, F. Han, X. Y. Zhu, and H.-H. Wen, e-print arXiv:1012.5637.

[28] A. Krzton-Maziopa, Z. Shermadini, E. Pomjakushina, V. Pomjakushin, M. Bendele, A. Amato, R. Khasanov, H. Luetkens, and K. Conder, J. Phys. Condens. Matter **23**, 052203 (2011).

[29] M. H. Fang, H. D. Wang, C. H. Dong, Z. J. Li, C. M. Feng, J. Chen, and H. Q. Yuan, e-print arXiv:1012.5236.

[30] B. Hunter, International Union of Crystallography Commission on Powder Diffraction Newsletter No. 20, 1998 [http://www.rietica.org].

[31] X. F. Wang, T. Wu, G. Wu, H. Chen, Y. L. Xie, J. J. Ying, Y. J. Yan, R. H. Liu, and X. H. Chen, Phys. Rev. Lett. **102**, 117005 (2009).

[32] J. Edwards and R. F. Frindt, J. Phys. Chem. Solids **32**, 2217 (1971).

[33] D. M. Wang, J. B. He, T.-L. Xia, and G. F. Chen, Phys. Rev. B **83**, 132502 (2011).

[34] H. D. Wang, C. H. Dong, Z. J. Li, S. S. Zhu, Q. H. Mao, C. M. Feng, H. Q. Yuan, and M. H. Fang, Europhys. Lett. **93**, 47004 (2011).

[35] X. G. Luo *et al.*, e-print arXiv:1101.5670.

[36] D. E. Prober, M. R. Beasley, and R. E. Schwall, Phys. Rev. B **15**, 5245 (1977).

[37] L. J. Li, X. D. Zhu, Y. P. Sun, H. C. Lei, B. S. Wang, S. B. Zhang, X. B. Zhu, Z. R. Yang, and W. H. Song, Physica C **470**, 313 (2010).

[38] H. C. Lei and C. Petrovic, e-print arXiv:1101.5616.

[39] G. M. Zhang, Y. H. Su, Z. Y. Lu, Z. Y. Weng, D. H. Lee, and T. Xiang, Europhys. Lett. **86**, 37006 (2009).

[40] K. Matan, R. Morinaga, K. Iida, and T. J. Sato, Phys. Rev. B **79**, 054526 (2009).

[41] C. Ren, Z. S. Wang, H. Q. Luo, H. Yang, L. Shan, and H. H. Wen, Physica C **469**, 599 (2009).

[42] H. Kupfer, I. Apfelstedt, R. Flúkiger, C. Keller, R. Meier-Hirmer, B. Runtsch, A. Turowski, U. Wiech, and T. Wolf, Cryogenics **28**, 650 (1988).

[43] C. Senatore, R. Flükiger, M. Cantoni, G. Wu, R. H. Liu, and X. H. Chen, Phys. Rev. B **78**, 054514 (2008).

[44] C. P. Bean, Phys. Rev. Lett. **8**, 250 (1962).

[45] E. M. Gyorgy, R. B. van Dover, K. A. Jackson, L. F. Schneemeyer, and J. V. Waszczak, Appl. Phys. Lett. **55**, 283 (1989).

[46] M. A. Tanatar, N. Ni, C. Martin, R. T. Gordon, H. Kim, V. G. Kogan, G. D. Samolyuk, S. L. Bud'ko, P. C. Canfield, and R. Prozorov, Phys. Rev. B **79**, 094507 (2009).